

**NOTE: This file includes two sections. Section 1 presents comments from the co-editor, referees, the corresponding point-by-point responses, and the related changes in the manuscript. Section 2 is the marked-up manuscript.**

**Section 1: (the black font are comments from the co-editor, referees, the red font are authors' responses as well as the related change clarifications.)**

**(1) Response to co-editor:**

Dear authors, the reviewers have made some recommendations for further minor revisions and corrections, please see the reports for details. Overall, the reviewers have commended you for the revisions already implemented and once the minor revisions are taken care of, we can proceed to publish the manuscript.

**Response:** This paper has been subjected to a minor revision/correction based on the comments from three referees. Detailed point-by-point response and the related changes are listed as follows:

**(2) Detailed response to comments from referee #1:**

Following the referee's remarks, the revised version has been strongly reorganized as compared to the initial version. As the authors state, (1) they have updated all retrievals with new  $S_a$  deduced from standard deviation of a dedicated WACCM run from 1980 to 2020, (2) they have organized the paper's structure, with focus on new results, and retaining only the most pertinent figures, (3) they omitted comparisons with the correlative data, i.e., OMI, GEOS-Chem and WRF-Chem data, (4) they reoriented the paper's focus on photochemical ozone regime. In my view, this responded to the major referee remarks, and makes the paper rather different from the initial one. I think, the paper shows now interesting results on data at a specific site and an interesting discussion of the ozone formation regime that can be deduced from the data. However, there is a major difficulty, because from reading the paper I think that the  $O_3$  product is not specific for PBL  $O_3$ , which would be needed for the current analysis. So I would think the paper is in principle worthwhile for publication in ACP, but only if this major issue is resolved or correctly addressed. Also figures should be better explained and a general rereading by a native speaker would be needed.

**Response:** Thanks very much for your recommendation with respect to publish this paper in ACP. Detailed explanations for your mentioned major issue are present, and we have tried our best to improve the language problem. I hope the ACP's copy and language editing service can fix the rest if we did not find out all of them.

In Section 3, it is not clear to me, what exactly are the altitude ranges of the partial columns that are the basis for the paper, and whether they are for the case of ozone pertinent, that is focusing on lower tropospheric ozone.

For instance, it is stated in section 3: “In this study, we have chosen the same upper limit for the tropospheric columns for all gases, which is about 3 km lower than the mean value of the tropopause (~15.1 km).” If I understand right, this means that 0 – 12 km partial columns are considered. But looking at figures S2 and S3, such columns would be sensitive to O<sub>3</sub> values up to 15 km. Following figure S3, wouldn't it be wiser to analyse a 0 – 8 km partial column being most sensitive between 0 and 6-8 km? This would allow being more sensitive to lower tropospheric ozone.

**Response:** Yes, for all gases, the tropospheric columns considered here are based on 0-12 km integration. In this way we ensured the accuracies for the tropospheric O<sub>3</sub>, CO, and HCHO retrievals, and minimized the influence of transport from stratosphere, i.e., the so called STE process (stratosphere-troposphere exchange). For O<sub>3</sub> and CO, as Figure S3 shown, it is wiser to analyse the 0 – 9 km partial column, which can reduce more STE influence and don't reduce much accuracies. However, for NO<sub>2</sub> and HCHO, the degrees of freedoms (DOFS) within 0-9 km is less than 1, and large uncertainty may arise. When taken everything into account, we selected 0 – 12 km partial column for all gases. On the other hand, as the following Figure 1 shows, there isn't much sensitivity difference between the 0-9 and 0-12km, and 0 – 12 km still holds most sensitivity on the lower tropospheric ozone. Actually, most previous studies even chosen the tropopause as the upper limit (Duncan et al., 2010; Choi et al., 2012; Witte et al., 2011; Jin and Holloway, 2015; Mahajan et al., 2015; Jin et al., 2017).

**Related change:** None

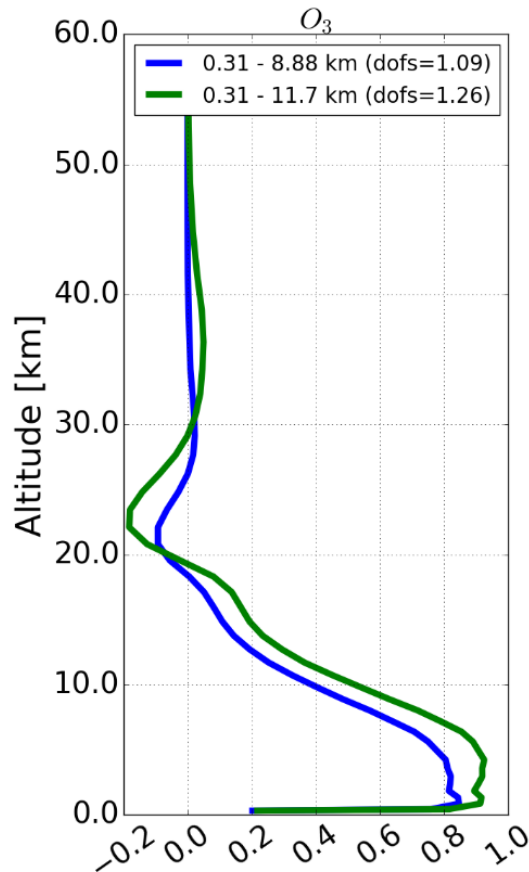


Figure 1. Partial column averaging kernels (PAVK) (ppmv / ppmv) for  $O_3$  in the troposphere. Anyway, it seems that  $O_3$  partial columns used here are heavily influenced, if not dominated by free tropospheric (FT) ozone located between, say, 2 – 8 km height. Note that it would be useful to dispose of boundary layer height values allowing to state where the FT begins. This important, if not dominant, FT part for ozone needs to be clearly stated in the paper, while in the current version, it is suggested that the analysed product is representative for PBL  $O_3$ . If authors think that their product has not only some fractional, but dominant information from the PBL, then please explain and prove it much better. Note that this applies for ozone, for  $NO_2$  and  $HCHO$ , the PBL sensitivity is stronger because both compounds are concentrated there.

If this suspected FT sensitivity is real, then the analysis needs to be taken into account in the following analysis. While PBL ozone can be strongly regionally controlled, FT ozone is prone to intercontinental or even hemispheric transport, including stratosphere – troposphere exchange. This needs to be addressed, and may be, the analysis completed or redirected. This point is really important to be addressed before

publication.

**Response:** Thanks very much for your useful and interesting comments. We hope the following statements can answer your questions.

1) Many scientists have proved that column technique (OMI, GOME, or airborne results) can be used to investigate PO<sub>3</sub> sensitivity, and the risky of the column technique was discussed in detail therein (Martin et al. 2004a; Duncan et al. 2010; Choi et al., 2012; Witte et al., 2011; Jin and Holloway, 2015; Mahajan et al., 2015; Schroeder et al., 2017; Jin et al., 2017). The NO<sub>2</sub> used in this study is the same as most previous studies, the sensitivity/resolution of FTS O<sub>3</sub> is close to that of OMI (Liu et al., 2010), the FTS HCHO is verified to be robust in troposphere in view of future satellite validation (Vigouroux et al., 2018). Thus, column technique used in this study is reasonable. We do acknowledge the paper by Schroeder et.al. (2017) which was published during the preparation of the manuscript. Schroeder et.al. (2017) question the usability of the column technique to infer PO<sub>3</sub> sensitivity. However, this manuscript does take into account much of the criticism mentioned by Schroeder et.al (2017): we calculated the transition thresholds with the measurements in Hefei rather than straightly applied the thresholds estimated by either previous studies. The FTIR measurements have a much smaller footprint than the satellite measurements. Also we concentrate on measurements recorded during midday, when the mixing layer has largely been dissolved. And furthermore, the measurements are more sensitive to the lower parts of the troposphere, which can be inferred from the normalized AVK's. This reason is simply, that the AVK's show the sensitivity to the column, but the column per altitude decreases with altitude.

2) Column measurements sample a larger portion of the atmosphere, and thus their spatial coverage are larger than in situ measurements. So the photochemical scene disclosed by column measurement is larger than the in-situ measurement. The retrieval in section 3 shows that the tropospheric DOFS of O<sub>3</sub> is only slightly larger than 1.0 (similar to previous studies which use tropospheric OMI product). O<sub>3</sub> retrieval does show large sensitivity in the troposphere, but is not sufficient to divided into PBL part and FT part. Generally, this study reflects the mean photochemical

condition of the troposphere.

3) In photochemical reaction, O<sub>3</sub> production is more sensitive to VOCs if it is VOCs-limited and is more sensitive to NO<sub>x</sub> if it is NO<sub>x</sub> limited, and it exists a transition point near the threshold (Martin et al., 2004). The transported ozone (e.g., STE process), if not produced by photochemical reaction, may alter tropospheric ozone amount but would not sensitive to either VOCs or NO<sub>x</sub>. Thus, it should not alter the photochemical regime estimated in this study. On the other hand, the selection of tropospheric limits 3 km below the tropopause minimized the influence of transport from stratosphere, the STE process.

**Related change:** We already included most of above explanation in the revised version.

Minor remarks:

Abstract :

Introduction:

“Briefly, VOCs first react with the hydroxyl radical (OH) to form a peroxy radical (HO<sub>2</sub>+ RO<sub>2</sub>) which increases the rate of catalytic cycling of NO to NO<sub>2</sub>. O<sub>3</sub> is then produced by subsequent reactions between HO<sub>2</sub>or RO<sub>2</sub> and NO that lead to radical propagation (via subsequent reformation of OH).

Please reformulate :

“Briefly, VOCs first react with the hydroxyl radical (OH) to form a peroxy radical (HO<sub>2</sub>+ RO<sub>2</sub>) which increases the rate of catalytic cycling of NO to NO<sub>2</sub>. O<sub>3</sub> is then produced by photolysis of NO<sub>2</sub>. Subsequent reactions between HO<sub>2</sub>or RO<sub>2</sub> and NO lead to radical propagation (via subsequent reformation of OH).

**Response:** This has been done.

Section 4.1:

“While it failed to determine the secular trend of tropospheric O<sub>3</sub> column probably because the time series is much shorter than those in Gardiner et al. (2008),”

This sentence suggests that the O<sub>3</sub> trend needs to be positive, but for later years, this is not necessarily the case, especially in the free troposphere.

**Response:** As suggested by reviewer#2, this sentence has been revised to “The

analysis did not indicate a significant secular trend of tropospheric O<sub>3</sub> column probably because the time series is much shorter than those in Gardiner et al. (2008).....”

#### Section 4.2

“The direction of east origin air masses shifts from the southeast to northeast of Jiangsu Province, and that of local origin air masses shifts from the south to the northwest of Anhui province.”

Please reformulate:

“The direction of air masses originating in the eastern sector shifts from the southeast to northeast of Jiangsu Province, and that of local air masses shifts from the south to the northwest of Anhui province.”

**Response:** This has been done.

“In contrast, trajectories of local origin air masses in SON/DJF are 20.2% larger than the MAM/JJA ones, indicating a more significant contribution of the air pollution inside Anhui province in SON/DJF.”

You mean, they are more frequent (instead of larger)?

**Response:** Yes, it is more frequent. In the revised version, the “larger” has been replaced by “more frequent”.

#### 5.1 Meteorological dependency

“The city downtown locates in eastern of the observation site and the majority of the Chinese population lives in the eastern part of China, easterly winds (direction less than 180°) could generally transport more pollutants to the observe area than westerly winds (direction larger than 180°), resulting in a higher O<sub>3</sub> level.”

This again supposes, that the O<sub>3</sub> product is mostly sensitive top PBL O<sub>3</sub>, which is clearly not proven. This also long range transport, not necessarily only from easterly regions, because trajectories can change directions, should contribute to enhanced O<sub>3</sub> columns.

**Response:** Since two referees worried/ puzzled about the wind data. We removed all wind data related panels and discussion. This sentence has been removed.

#### Section 5.2 :

“Pronounced tropospheric CO and NO<sub>2</sub> variations were observed but the seasonal cycles are not evident probably because of air pollution which is not constant over season or season dependent.”

This is not clear. For NO<sub>2</sub> a winter maximum is found. One reason is that time series are not complete enough especially in the later years.

**Response:** It has been changed to “Generally, tropospheric HCHO are higher and tropospheric NO<sub>2</sub> are lower in MAM/JJA than those in SON/DJF. Pronounced tropospheric CO was observed but the seasonal cycle is not evident probably because CO emission is not constant over season or season dependent.”

“Since the sensitivity of PO<sub>3</sub> to VOCs and NO<sub>x</sub> is different under different limitation regimes, the relative weaker overall correlations to HCHO (Figure 6 (b)) and NO<sub>2</sub> (Figure 6 (c)) indicates that the O<sub>3</sub> pollution in Hefei can neither be fully attributed to NO<sub>x</sub> pollution nor VOCs pollution.”

If O<sub>3</sub> columns are representative for PBL, then weaker correlation of O<sub>3</sub> with NO<sub>2</sub> and HCHO are also explained by different lifetimes, hours to 1 day in summer for NO<sub>2</sub> and HCHO, several days to weeks for O<sub>3</sub>. So older O<sub>3</sub> enhanced air masses easily loose trace of NO<sub>2</sub> or HCHO. Please add this explanation. If they are dominated by FT O<sub>3</sub>, then a correlation can not be expected anyway. This seems to be the case.

**Response:** We have included this explanation in the revised version.

Figure 1:

In figure 1, how is the trend calculated? how are the points named ‘resampled bootstrap’ obtained. Please explain in the text.

**Response:** Since the method is already described in detail in Gardiner et al., 2008. We included this reference in the text to avoid repetition.

Figure 3 :

Monthly average wind speed of 0 does not make sense, as already stated by another referee. It is understood that the average of absolute wind speed is meant. If you cannot calculate it, please withdraw this figure. Also the figure on wind direction on wind direction is not easy to interpret. May be a solution is to calculate frequency distributions.

**Response:** Since two referees worried/ puzzled about the wind data. We removed all wind data related panels and discussion.

Figure 4:

If minute average FTS measurements are used, then there should be much more points?  
Or do you use time averages?

**Response:** The FTS retrievals within  $\pm 30$  min of OMI overpass time (13:30 local time (LT)) were averaged and used in this study.

**Related change:** We included this statement in the introduction (last paragraph).

Figure 5 and Figure 6: again, what is the measurement period one point corresponds to ?

**Response:** The FTS retrievals within  $\pm 30$  min of OMI overpass time (13:30 local time (LT)) were averaged and used in this study.

**Related change:** We included this statement in the introduction (last paragraph).

Supplement:

“FigureS2. Averaging kernels(ppmv/ppmv)of O<sub>3</sub>, CO, and HCHO (color fine lines), and their area scaled by a factor of 0.2 (black bold line).They are deduced from the spectra recorded in Hefei on March 15, 2016 with a measured ILS.”

Please clarify several points in the figures legend. Each curve is representative for 1 km ? What does the area curve exactly indicate? what does “ILS” stand for ?

**Response:** ILS stands for instrumental line shape. The atmosphere (0 – 120 km) is unevenly divided into 48 layers, and each curve corresponds to one layer which is not exactly for 1 km.

**Related change:** We have clarified several points in the figures legend.

“FigureS3. Partial column averaging kernels(PAVK)(ppmv/ppmv) for O<sub>3</sub>, CO, and HCHO retrievals. For all gases, large PAVKs in certain altitude range”

Are the PAVK’s obtained by summing up the km wise AVK’s ?

**Response:** Yes, PAVK’s are obtained by summing up the concerned km AVK’s.

### (3) Detailed response to comments from referee #2:

The authors have revised the manuscript quite extensively and have addressed many of the concerns raised by the reviewers. The manuscript now has a much clearer



message and storyline. The questionable comparisons to other observations and model simulations have been removed from the previous version. I think that this is now publishable in the ACP special edition, after a few mostly minor revisions.

**Response:** Thanks very much for your recommendation with respect to publish this paper in ACP. All glitches listed by you have been addressed. Please check details as below.

Generally, the English should be improved throughout the manuscript, especially in the later sections. I assume that much of this will be done in the copy-editing phase.

**Response:** We have tried our best to improve the language problem. I hope the ACP's copy and language editing service can fix the rest if we did not find out all of them.

line 22: I would delete "different". I think "and modelling" also needs to be deleted, because modelling is not really used anymore in the revised version.

**Response:** "different" and "and modelling" have been removed.

lines 30,31 (and 232,233; 452,453): I find this awkward. Why not state the June value  $1.5 \times 10^{18}$ ? Given the variations and uncertainties 47.6% should probably be 50%. It would also be useful to give these column densities in Dobson Units (DU):  $1.5 \times 10^{18} / \text{cm}^2 = 56 \text{ DU}$ ,  $1.05 \times 10^{18} / \text{cm}^2 = 39 \text{ DU}$

**Response:** As your suggestion, these sentence have been changed to “ Tropospheric O<sub>3</sub> columns in June are  $1.55 \times 10^{18}$  molecules\*cm<sup>-2</sup> (56 DU (Dobson Units)) and in December are  $1.05 \times 10^{18}$  molecules\*cm<sup>-2</sup> (39 DU). Tropospheric O<sub>3</sub> columns in June were ~ 50% higher than those in December.”

lines 32 to 35: This sentence does not make sense to me. MAM/JJA is mainly influence by transport whereas MAM/JJA is mostly determined by photochemical production? Please rethink and reword.

**Response:** Has been changed to “Compared with SON/DJF season, the observed tropospheric O<sub>3</sub> levels in MAM/JJA are more influenced by transport of air masses from densely populated and industrialized areas, and the high O<sub>3</sub> level and variability in MAM/JJA is determined by the photochemical O<sub>3</sub> production.”

line 40: % of what? Probably "of days" or "of cases". Change as appropriate.

**Response:** has been revised to “% of days”

line 42: delete "most of the". This has not been shown.

**Response:** "most of the" has been removed.

line 222: I would replace "failed to determine the" by something like "the analysis did not indicate a significant"

**Response:** has been replaced by " the analysis did not indicate a significant..... " .

line 229: delete "it shows that"

**Response:** has been done.

lines 237 to 240: Not really true. Izana also shows an early summer maximum in May, at a latitude not too different from Hefei. Somewhere, you should also state that the tropospheric columns at these stations are of the order of  $0.7 \times 10^{18} \text{ cm}^{-2}$  to  $1.1 \times 10^{18} \text{ cm}^{-2}$ , around 30% lower than at Hefei.

**Response:** "The tropospheric columns at these stations are of the order of  $0.7 \times 10^{18}$  molecules\* $\text{cm}^{-2}$  to  $1.1 \times 10^{18}$  molecules\* $\text{cm}^{-2}$ , around 30% lower than at Hefei." and "The results showed a maximum tropospheric O<sub>3</sub> column in spring at all these stations except at the high altitude stations Jungfraujoch and Izaña where it extended into early summer." have been included in the revised version.

lines 249 to 251: I find this sentence confusing and I suggest to omit it.

**Response:** This sentence has been removed.

line 262, and throughout section 4.2.: In most cases "air pollution" should be replaced by "air masses". The trajectory does not tell you anything about air pollution and its photo-chemical effects. It just tells you where the air masses (might) come from. Everything else is assumptions and plausibility.

**Response:** This has been done in the revised version.

line 276: Replace "dominate the contribution" by "contributes". Without a quantitative analysis, you do not know what dominates.

**Response:** This has been done in the revised version.

line 277: Replace "masses" by "trajectories".

**Response:** This has been done in the revised version.

line 282: replace "smaller" by "less frequent"

**Response:** This has been done in the revised version.

line 300: delete "which can be"

**Response:** This has been done in the revised version.

lines 308 to 318, Figs. 3 and 4: I am a bit worried/ puzzled about the wind data. Wind direction seems to be all over the place, and wind speeds seems to vary greatly between minutes and hours. Where do these short wind gusts come from? How representative is the local scale weather-station wind for the tropospheric FTIR columns? It might be much better to use larger scale winds, e.g. from the GDAS data? I think the wind data in Figs. 3 and 4 need careful checking, and it may be necessary to change or drop these panels and their discussion.

**Response:** Since two referees worried/ puzzled about the wind data. We removed all wind data related panels and discussion.

lines 339, 340: Something wrong with that sentence. Please fix.

**Response:** Has been revised to "Figure 5 shows time series of tropospheric CO, HCHO, and NO<sub>2</sub> columns that are coincident with O<sub>3</sub> counterparts....."

lines 368 to 385: I don't think any of this information is needed here, and I find it more confusing than helpful. I suggest to drop this text.

**Response:** All these information have been removed.

lines 414 to 423: So this study finds a VOC - NO<sub>x</sub> transition regime at HCHO/NO<sub>x</sub> ratios between 1.3 and 2.8, whereas previous (in situ based) studies found it at HCHO/NO<sub>x</sub> ratios between 1 and 2. I think this is pretty good agreement and could be emphasized. You point out that your study is not in-situ, and this could explain some differences. Could you please also add a statement about possible chemical differences?

**Response:** Duncan et al. (2010) concluded that O<sub>3</sub> production decreases with reductions in VOCs at column HCHO/NO<sub>2</sub> ratio < 1.0 and NO<sub>x</sub> at column HCHO/NO<sub>2</sub> ratio > 2.0; both NO<sub>x</sub> and VOCs reductions decrease O<sub>3</sub> production when column HCHO/NO<sub>2</sub> ratio lies in between 1.0 and 2.0. This means, HCHO/NO<sub>x</sub> ratios between 1 and 2 is also based on tropospheric column technique and not from in-situ. Regarding the possible chemical difference between in situ and column measurement can be found in previous studies like Choi et al., 2012; Witte et al., 2011; Jin and

Holloway, 2015; Mahajan et al., 2015; Jin et al., 2017 or Schroeder et al. 2017. Briefly, column measurements sample a larger portion of the atmosphere, and thus their spatial coverage are larger than in situ measurements. So the photochemical scene disclosed by column measurement is larger than the in-situ measurement.

**Response:** We have include this statement about possible chemical differences in section 5.3.2.

**(4) Detailed response to comments from referee #3:**

The paper documents retrievals of ozone, formaldehyde, and carbon monoxide using FTS observations in the central portion of eastern China over the 2014-2017 period. The paper also provides some reasonable analysis of the sources of the ozone values at this station. I read the revised version, and went back and looked over the original version. First, the authors have put in a nice effort into revising their manuscript and mainly responding to the critiques of the original manuscript. Second, the discussion on the retrievals, kernels, uncertainties is well done. I would rate my confidence in the data and retrievals to be quite high. Third, tropospheric chemistry in not my forte, but I'm skeptical of inferring information from column observations. Since ozone production is a non-linear function of VOCs and NO<sub>x</sub>, and since much of this is found in the boundary layer or strong plumes in the free troposphere, it is difficult to inter much information from column observations. Hence, I find some of the correlations shown in the manuscript to be not well founded or poor. Hence, the overall analysis is marginal in my "dynamicist" view. Nevertheless, this is interesting data from a highly polluted region that should be in the literature. Hence, I feel this should be published.

**Response:** Thanks very much for your recommendation with respect to publish this paper in ACP. Regarding your skeptical of inferring information from column observations, here are our explanations:

1) Column measurements sample a larger portion of the atmosphere, and thus their spatial coverage are larger than in situ measurements. So the photochemical scene disclosed by column measurement is larger than the in-situ measurement. The retrieval in section 3 shows that the tropospheric DOFS of O<sub>3</sub> is only slightly larger than 1.0 (similar to previous studies which use tropospheric OMI product). O<sub>3</sub>

retrieval does show large sensitivity in the troposphere, but is not sufficient to divided into PBL part and FT part. Generally, this study reflects the mean photochemical condition of the troposphere.

2) Many scientists have proved that column technique (OMI, GOME, or airborne results) can be used to investigate  $\text{PO}_3$  sensitivity, and the risky of the column technique was discussed in detail therein (Martin et al. 2004a; Duncan et al. 2010; Choi et al., 2012; Witte et al., 2011; Jin and Holloway, 2015; Mahajan et al., 2015; Schroeder et al., 2017; Jin et al., 2017). The  $\text{NO}_2$  used in this study is the same as most previous studies, the sensitivity/resolution of FTS  $\text{O}_3$  is close to that of OMI (Liu et al., 2010), the FTS HCHO is verified to be robust in troposphere in view of future satellite validation (Vigouroux et al., 2018). Thus, column technique used in this study is reasonable. We do acknowledge the paper by Schroeder et.al. (2017) which was published during the preparation of the manuscript. Schroeder et.al. (2017) question the usability of the column technique to infer  $\text{PO}_3$  sensitivity. However, this manuscript does take into account much of the criticism mentioned by Schroeder et.el (2017): we calculated the transition thresholds with the measurements in Hefei rather than straightly applied the thresholds estimated by either previous studies. The FTIR measurements have a much smaller footprint than the satellite measurements. Also we concentrate on measurements recorded during midday, when the mixing layer has largely been dissolved. And furthermore, the measurements are more sensitive to the lower parts of the troposphere, which can be inferred from the normalized AVK's. This reason is simply, that the AVK's show the sensitivity to the column, but the column per altitude decreases with altitude.

**In detail:** Over polluted areas, both HCHO and tropospheric  $\text{NO}_2$  have vertical distributions that are heavily weighted toward the lower troposphere, indicating that tropospheric column measurements of these gases are fairly representative of near surface conditions. Many studies have taken advantage of these favorable vertical distributions to investigate surface emissions of  $\text{NO}_x$  and VOCs from space (Boersma et al., 2009; Martin et al., 2004a; Millet et al., 2008; Streets et al., 2013). Martin et al. (2004a) and Duncan et al. (2010) used satellite measurements of column HCHO/ $\text{NO}_2$

ratio to explore tropospheric O<sub>3</sub> sensitivities from space and disclosed that this diagnosis of O<sub>3</sub> production rate (PO<sub>3</sub>) is consistent with previous finding of surface photochemistry. Witte et al. (2011) used a similar technique to estimate changes in PO<sub>3</sub> to the strict emission control measures (ECMs) during Beijing Summer Olympic Games period in 2008. Recent papers have applied the findings of Duncan et al. (2010) to observe O<sub>3</sub> sensitivity in other parts of the world (Choi et al., 2012; Witte et al., 2011; Jin and Holloway, 2015; Mahajan et al., 2015; Schroeder et al., 2017; Jin et al., 2017).

## **Section 2: marked up file, as follows**

In briefly, we have moved all wind data related panels in Figs. 3 and 4, and the corresponding discussion in section 5.1. Other minor revisions responded to referees' comments also performed. We have tried our best to improve the language problem. The marked up file is as follow, please check the red underlined sentences for details:

### **Ozone seasonal evolution and photochemical production regime in polluted troposphere in eastern China derived from high resolution FTS observations**

Youwen Sun <sup>1, 2) #</sup>, Cheng Liu <sup>2, 3, 1) #<sup>1</sup></sup>, Mathias Palm <sup>4)</sup>, Corinne Vigouroux <sup>5)</sup>, Justus Notholt <sup>4)</sup>, Qihou Hu <sup>1)</sup>, Nicholas Jones <sup>6)</sup>, Wei Wang <sup>1)</sup>, Wenjing Su <sup>3)</sup>, Wenqiang Zhang <sup>3)</sup>, Changong Shan <sup>1)</sup>, Yuan Tian <sup>1)</sup>, Xingwei, Xu <sup>1)</sup>, Martine De Mazière <sup>5)</sup>, Minqiang Zhou <sup>5)</sup>, and Jianguo Liu <sup>1)</sup>

*(1 Key Laboratory of Environmental Optics and Technology, Anhui Institute of Optics and Fine Mechanics, Chinese Academy of Sciences, Hefei 230031, China)*

*(2 Center for Excellence in Urban Atmospheric Environment, Institute of Urban Environment, Chinese Academy of Sciences, Xiamen 361021, China)*

*(3 University of Science and Technology of China, Hefei, 230026, China)*

*(4 University of Bremen, Institute of Environmental Physics, P. O. Box 330440, 28334 Bremen, Germany)*

*(5 Royal Belgian Institute for Space Aeronomy (BIRA-IASB), Brussels, Belgium)*

*(6 School of Chemistry, University of Wollongong, Northfields Ave, Wollongong, NSW,*

---

Correspondence to: Cheng Liu ([chliu81@ustc.edu.cn](mailto:chliu81@ustc.edu.cn)) or Youwen Sun ([ywsun@aiofm.ac.cn](mailto:ywsun@aiofm.ac.cn))

2522, Australia )

# These two authors contributed equally to this work

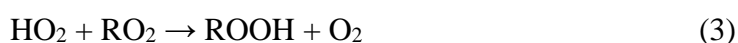
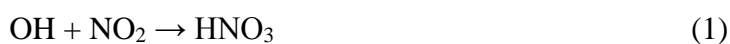
## **Abstract:**

The seasonal evolution of O<sub>3</sub> and its photochemical production regime in a polluted region of eastern China between 2014 and 2017 has been investigated using [observations](#). We used tropospheric ozone (O<sub>3</sub>), carbon monoxide (CO) and formaldehyde (HCHO, a marker of VOCs (volatile organic compounds)) partial columns derived from high resolution Fourier transform spectrometry (FTS), tropospheric nitrogen dioxide (NO<sub>2</sub>, a marker of NO<sub>x</sub> (nitrogen oxides)) partial column deduced from Ozone Monitoring Instrument (OMI), surface meteorological data, and a back trajectory cluster analysis technique. A broad O<sub>3</sub> maximum during both spring and summer (MAM/JJA) is observed; the day-to-day variations in MAM/JJA are generally larger than those in autumn and winter (SON/DJF). Tropospheric O<sub>3</sub> columns in June are  $1.55 \times 10^{18}$  molecules\*cm<sup>-2</sup> ([56 DU \(Dobson Units\)](#)) and in December are  $1.05 \times 10^{18}$  molecules\*cm<sup>-2</sup> ([39 DU](#)). [Tropospheric O<sub>3</sub> columns in June were ~ 50% higher than those in December](#). Compared with SON/DJF season, the observed tropospheric O<sub>3</sub> levels in MAM/JJA are [more](#) influenced by transport of air masses from densely populated and industrialized areas, and the [high O<sub>3</sub> level and variability](#) in MAM/JJA is determined by the photochemical O<sub>3</sub> production. The tropospheric column HCHO/NO<sub>2</sub> ratio is used as a proxy to investigate the photochemical O<sub>3</sub> production rate (PO<sub>3</sub>). The results show that the PO<sub>3</sub> is mainly nitrogen oxides (NO<sub>x</sub>) limited in MAM/JJA, while it is mainly VOC or mix VOC-NO<sub>x</sub> limited in SON/DJF. Statistics show that NO<sub>x</sub> limited, mix VOC-NO<sub>x</sub> limited, and VOC limited PO<sub>3</sub> accounts for 60.1%, 28.7%, and 11% [of days](#), respectively. Considering most of PO<sub>3</sub> are NO<sub>x</sub> limited or mix VOC-NO<sub>x</sub> limited, reductions in NO<sub>x</sub> would [reduce](#) O<sub>3</sub> pollution in eastern China.

## **1 Introduction**

Human health, terrestrial ecosystems, and materials degradation are impacted by poor air quality resulting from high photochemical ozone (O<sub>3</sub>) levels (Wennberg and

Dabdub, 2008; Edwards et al., 2013; Schroeder et al., 2017). In polluted areas, tropospheric O<sub>3</sub> generates from a series of complex reactions in the presence of sunlight involving carbon monoxide (CO), nitrogen oxides (NO<sub>x</sub> ≡ NO (nitric oxide) + NO<sub>2</sub> (nitrogen dioxide)), and volatile organic compounds (VOCs) (Oltmans et al., 2006; Schroeder et al., 2017). Briefly, VOCs first react with the hydroxyl radical (OH) to form a peroxy radical (HO<sub>2</sub> + RO<sub>2</sub>) which increases the rate of catalytic cycling of NO to NO<sub>2</sub>. O<sub>3</sub> is then produced by photolysis of NO<sub>2</sub>. Subsequent reactions between HO<sub>2</sub> or RO<sub>2</sub> and NO lead to radical propagation (via subsequent reformation of OH). Radical termination proceeds via reaction of OH with NO<sub>x</sub> to form nitric acid (HNO<sub>3</sub>) (reaction (1), referred to as LNO<sub>x</sub>) or by radical-radical reactions resulting in stable peroxide formation (reactions (2) – (4), referred to as LRO<sub>x</sub>, where RO<sub>x</sub> ≡ RO<sub>2</sub> + HO<sub>2</sub>) (Schroeder et al., 2017):



Typically, the relationship between these two competing radical termination processes (referred to as the ratio LRO<sub>x</sub>/LNO<sub>x</sub>) can be used to evaluate the photochemical regime. In high-radical, low-NO<sub>x</sub> environments, reactions (2) – (4) remove radicals at a faster rate than reaction (1) (i.e., LRO<sub>x</sub> ≫ LNO<sub>x</sub>), and the photochemical regime is regarded as “NO<sub>x</sub> limited”. In low-radical, high-NO<sub>x</sub> environments the opposite is true (i.e., LRO<sub>x</sub> ≪ LNO<sub>x</sub>) and the regime is regarded as “VOC limited”. When the rates of the two loss processes are comparable (LNO<sub>x</sub> ≈ LRO<sub>x</sub>), the regime is said to be at the photochemical transition/ambiguous point, i.e., mix VOC-NO<sub>x</sub> limited (Kleinman et al., 2005; Sillman et al., 1995a; Schroeder et al., 2017).

Understanding the photochemical regime at local scales is a crucial piece of information for enacting effective policies to mitigate O<sub>3</sub> pollution (Jin et al., 2017; Schroeder et al., 2017). In order to determine the regime, the total reactivity with OH of the myriad of VOCs in the polluted area has to be estimated (Sillman, 1995a; Xing et al., 2017). In the absence of such information, the formaldehyde (HCHO)



concentration can be used as a proxy for VOC reactivity because it is a short-lived oxidation product of many VOCs and is positively correlated with peroxy radicals (Schroeder et al., 2017). Sillman (1995a) and Tonnesen and Dennis (2000) found that in situ measurements of the ratio of HCHO (a marker of VOCs) to NO<sub>2</sub> (a marker of NO<sub>x</sub>) could be used to diagnose local photochemical regimes. Over polluted areas, both HCHO and tropospheric NO<sub>2</sub> have vertical distributions that are heavily weighted toward the lower troposphere, indicating that tropospheric column measurements of these gases are fairly representative of near surface conditions. Many studies have taken advantage of these favorable vertical distributions to investigate surface emissions of NO<sub>x</sub> and VOCs from space (Boersma et al., 2009; Martin et al., 2004a; Millet et al., 2008; Streets et al., 2013). Martin et al. (2004a) and Duncan et al. (2010) used satellite measurements of column HCHO/NO<sub>2</sub> ratio to explore tropospheric O<sub>3</sub> sensitivities from space and disclosed that this diagnosis of O<sub>3</sub> production rate (PO<sub>3</sub>) is consistent with previous finding of surface photochemistry. Witte et al. (2011) used the similar technique to estimate changes in PO<sub>3</sub> to the strict emission control measures (ECMs) during Beijing Summer Olympic Games period in 2008. Recent papers have applied the findings of Duncan et al. (2010) to observe O<sub>3</sub> sensitivity in other parts of the world (Choi et al., 2012; Witte et al., 2011; Jin and Holloway, 2015; Mahajan et al., 2015; Jin et al., 2017).

With in situ measurements, Tonnesen and Dennis (2000) observed a radical-limited environment with HCHO/NO<sub>2</sub> ratios < 0.8, a NO<sub>x</sub>-limited environment with HCHO/NO<sub>2</sub> ratios >1.8, and a transition environment with HCHO/NO<sub>2</sub> ratios between 0.8 and 1.8. With 3-d chemical model simulations, Sillman (1995a) and Martin et al. (2004b) estimated that the transition between the VOC- and NO<sub>x</sub>-limited regimes occurs when the HCHO/NO<sub>2</sub> ratio is ~ 1.0. With a combination of regional chemical model simulations and the Ozone Monitoring Instrument (OMI) measurements, Duncan et al. (2010) concluded that O<sub>3</sub> production decreases with reductions in VOCs at column HCHO/NO<sub>2</sub> ratio < 1.0 and NO<sub>x</sub> at column HCHO/NO<sub>2</sub> ratio > 2.0; both NO<sub>x</sub> and VOCs reductions decrease O<sub>3</sub> production when column HCHO/NO<sub>2</sub> ratio lies in between 1.0 and 2.0. With a 0-D

photochemical box model and airborne measurements, Schroeder et al. (2017) presented a thorough analysis of the utility of column HCHO/NO<sub>2</sub> ratios to indicate surface O<sub>3</sub> sensitivity and found that the transition/ambiguous range estimated via column data is much larger than that indicated by in situ data alone. Furthermore, Schroeder et al. (2017) concluded that many additional sources of uncertainty (regional variability, seasonal variability, variable free tropospheric contributions, retrieval uncertainty, air pollution levels and meteorological conditions) may cause transition threshold vary both geographically and temporally, and thus the results from one region are not likely to be applicable globally.

With the rapid increase in fossil fuel consumption in China over the past three decades, the emission of chemical precursors of O<sub>3</sub> (NO<sub>x</sub> and VOCs) has increased dramatically, surpassing that of North America and Europe and raising concerns about worsening O<sub>3</sub> pollution in China (Tang et al., 2011; Wang et al., 2017; Xing et al., 2017). Tropospheric O<sub>3</sub> was already included in the new air quality standard as a routine monitoring component (<http://www.mep.gov.cn>, last access on 23 May 2018), where the limit for the maximum daily 8 h average (MDA8) O<sub>3</sub> in urban and industrial areas is 160 μg/m<sup>3</sup> (~ 75 ppbv at 273 K, 101.3 kPa). According to air quality data released by the Chinese Ministry of Environmental Protection, tropospheric O<sub>3</sub> has replaced PM<sub>2.5</sub> as the primary pollutant in many cities during summer (<http://www.mep.gov.cn/>, last access on 23 May 2018). A precise knowledge of O<sub>3</sub> evolution and photochemical production regime in polluted troposphere in China has important policy implications for O<sub>3</sub> pollution controls (Tang et al., 2011; Xing et al., 2017; Wang et al., 2017).

In this study, we investigate O<sub>3</sub> seasonal evolution and photochemical production regime in the polluted troposphere in eastern China with tropospheric O<sub>3</sub>, CO and HCHO derived from ground-based high resolution Fourier transform spectrometry (FTS) in Hefei, China, tropospheric NO<sub>2</sub> deduced from the OMI satellite (<https://aura.gsfc.nasa.gov/omi.html>, last access on 23 May 2018), surface meteorological data, and a back trajectory cluster analysis technique. Considering the fact that most NDACC (Network for Detection of Atmospheric Composition Change)

FTS sites are located in Europe and Northern America, whereas the number of sites in Asia, Africa, and South America is very sparse, and there is still no official NDACC FTS station that covers China (<http://www.ndacc.org/>, last access on 23 May 2018), this study can not only improve our understanding of regional photochemical O<sub>3</sub> production regime, but also contributes to the evaluation of O<sub>3</sub> pollution controls.

This study concentrates on measurements recorded during midday, when the mixing layer has largely been dissolved. All FTS retrievals are selected within  $\pm 30$  min of OMI overpass time (13:30 local time (LT)). While the FTS instrument can measure throughout the whole day, if not cloudy, OMI measures only during midday. For Hefei, this coincidence criterion is a balance between the accuracy and the number of data points.

## **2 Site description and instrumentation**

The FTS observation site (117°10'E, 31°54'N, 30 m a.s.l. (above sea level)) is located in the western suburbs of Hefei city (the capital of Anhui Province, 8 million population) in central-eastern China (Figure S1). Detailed description of this site and its typical observation scenario can be found in Tian et al. (2018). Similar to other Chinese megacities, serious air pollution is common in Hefei throughout the whole year (<http://mep.gov.cn/>, last access on 23 May 2018).

Our observation system consists of a high resolution FTS spectrometer (IFS125HR, Bruker GmbH, Germany), a solar tracker (Tracker-A Solar 547, Bruker GmbH, Germany), and a weather station (ZENO-3200, Coastal Environmental Systems, Inc., USA). The near infrared (NIR) and middle infrared (MIR) solar spectra were alternately acquired in routine observations (Wang et al., 2017). The MIR spectra used in this study are recorded over a wide spectral range (about 600 – 4500 cm<sup>-1</sup>) with a spectral resolution of 0.005cm<sup>-1</sup>. The instrument is equipped with a KBr beam splitter & MCT detector for O<sub>3</sub> measurements and a KBr beam splitter & InSb detector for other gases. The weather station includes sensors for air pressure ( $\pm 0.1$ hpa), air temperature ( $\pm 0.3$  °C), relative humidity ( $\pm 3\%$ ), solar radiation ( $\pm 5\%$ ), wind speed ( $\pm 0.2$  m/s), wind direction ( $\pm 5$  °), and the presence of rain.

## 3 FTS retrievals of O<sub>3</sub>, CO and HCHO

### 3.1 Retrieval strategy

The SFIT4 (version 0.9.4.4) algorithm is used in the profile retrieval (Supplement section A; <https://www2.acom.ucar.edu/irwg/links>, last access on 23 May 2018). The retrieval settings for O<sub>3</sub>, CO, and HCHO are listed in Table 1. All spectroscopic line parameters are adopted from HITRAN 2008 (Rothman et al., 2009). A priori profiles of all gases except H<sub>2</sub>O are from a dedicated WACCM (Whole Atmosphere Community Climate Model) run. A priori profiles of pressure, temperature and H<sub>2</sub>O are interpolated from the National Centers for Environmental Protection and National Center for Atmospheric Research (NCEP/NCAR) reanalysis (Kalnay et al., 1996). For O<sub>3</sub> and CO, we follow the NDACC standard convention with respect to micro windows (MW) selection and the interfering gases consideration (<https://www2.acom.ucar.edu/irwg/links>, last access on 23 May 2018). HCHO is not yet an official NDACC species but has been retrieved at a few stations with different retrieval settings (Albrecht et al., 2002; Vigouroux et al., 2009; Jones et al., 2009; Viatte et al., 2014; Franco et al., 2015). The four MWs used in the current study are chosen from a harmonization project taking place in view of future satellite validation (Vigouroux et al., 2018). They are centered at around 2770 cm<sup>-1</sup> and the interfering gases are CH<sub>4</sub>, O<sub>3</sub>, N<sub>2</sub>O, and HDO.

We assume measurement noise covariance matrices  $\mathbf{S}_e$  to be diagonal, and set its diagonal elements to the inverse square of the signal to noise ratio (SNR) of the fitted spectra and its non-diagonal elements to zero. For all gases, the diagonal elements of *a priori* profile covariance matrices  $\mathbf{S}_a$  are set to standard deviation of a dedicated WACCM run from 1980 to 2020, and its non-diagonal elements are set to zero.

We regularly used a low-pressure HBr cell to monitor the instrument line shape (ILS) of the instrument and included the measured ILS in the retrieval (Hase et al., 2012; Sun et al., 2018).

### 3.2 Profile information in the FTS retrievals

The sensitive range for CO and HCHO is mainly tropospheric, and for O<sub>3</sub> is both tropospheric and stratospheric (Figure S2). The typical degrees of freedom (DOFS) over the total atmosphere obtained at Hefei for each gas are included in Table 2: they are about 4.8, 3.5, and 1.2 for O<sub>3</sub>, CO, and HCHO, respectively. In order to separate

independent partial column amounts in the retrieved profiles, we have chosen the altitude limit for each independent layer such that the DOFS in each associated partial column is not less than 1.0. The retrieved profiles of O<sub>3</sub>, CO, and HCHO can be divided into four, three, and one independent layers, respectively (Figure S3). The troposphere is well resolved by O<sub>3</sub>, CO, and HCHO, where CO exhibits the best vertical resolution with more than two independent layers in the troposphere.

In this study, we have chosen the same upper limit ([12 km](#)) for the tropospheric columns for all gases ([Table 2](#)), which is about 3 km lower than the mean value of the tropopause (~15.1 km). In this way we ensured the accuracies for the tropospheric O<sub>3</sub>, CO, and HCHO retrievals, and minimized the influence of transport from stratosphere, i.e., the so called STE process (stratosphere-troposphere exchange).

### 3.3 Error analysis

The results of the error analysis presented here based on the average of all measurements that fulfill the screening scheme, which is used to minimize the impacts of significant weather events or instrument problems (Supplement section B). In the troposphere, the dominant systematic error for O<sub>3</sub> and CO is the smoothing error, and for HCHO is the line intensity error (Figure S4). The dominant random error for O<sub>3</sub> and HCHO is the measurement error, and for CO is the zero baseline level error (Figure S5). Taken all error items into account, the summarized errors in O<sub>3</sub>, CO, and HCHO for 0–12 km tropospheric partial column and for the total column are listed in Table 3. The total errors in the tropospheric partial columns for O<sub>3</sub>, CO, and HCHO, have been evaluated to be 8.7%, 6.8%, and 10.2%, respectively.

## 4 Tropospheric O<sub>3</sub> seasonal evolution

### 4.1 Tropospheric O<sub>3</sub> seasonal variability

Figure 1(a) shows the tropospheric O<sub>3</sub> column time series recorded by the FTS from 2014 to 2017, where we followed Gardiner's method and used a second-order Fourier series plus a linear component to determine the annual variability (Gardiner et al., 2008). The analysis did not indicate a [significant secular trend](#) of tropospheric O<sub>3</sub> column probably because the time series is much shorter than those in Gardiner et al. (2008), the observed seasonal cycle of tropospheric O<sub>3</sub> variations is well captured by the bootstrap resampling method (Gardiner et al., 2008). As commonly observed, high

levels of tropospheric O<sub>3</sub> occur in spring and summer (hereafter MAM/JJA). Low levels of tropospheric O<sub>3</sub> occur in autumn and winter (hereafter SON/DJF). Day-to-day variations in MAM/JJA are generally larger than those in SON/DJF (Figure 1(b)). At the same time, the tropospheric O<sub>3</sub> column roughly increases over time at the first half of the year and reaches the maximum in June, and then decreases during the second half of the year. Tropospheric O<sub>3</sub> columns in June are  $1.55 \times 10^{18}$  molecules\*cm<sup>-2</sup> (56 DU (Dobson Units)) and in December are  $1.05 \times 10^{18}$  molecules\*cm<sup>-2</sup> (39 DU). Tropospheric O<sub>3</sub> columns in June were ~ 50% higher than those in December.

Vigouroux et al. (2015) studied the O<sub>3</sub> trends and variabilities at eight NDACC FTS stations that have a long-term time series of O<sub>3</sub> measurements, namely, Ny-Ålesund (79 °N), Thule (77 °N), Kiruna (68 °N), Harestua (60 °N), Jungfraujoch (47 °N), Izaña (28 °N), Wollongong (34 °S) and Lauder (45 °S). All these stations were located in non-polluted or relatively clean areas. The tropospheric columns at these stations are of the order of  $0.7 \times 10^{18}$  molecules\*cm<sup>-2</sup> to  $1.1 \times 10^{18}$  molecules\*cm<sup>-2</sup>. The results showed a maximum tropospheric O<sub>3</sub> column in spring at all these stations except at the high altitude stations Jungfraujoch and Izaña where it extended into early summer. This is because the STE process is most effective during late winter and spring (Vigouroux et al. 2015). In contrast, we observed a broader maximum at Hefei which extends over MAM/JJA season, and the values are ~ 35% higher than those studied in Vigouroux et al. (2015). This is because the observed tropospheric O<sub>3</sub> levels in MAM/JJA are more influenced by air masses originated from densely populated and industrialized areas (see section 4.2), and the MAM/JJA meteorological conditions are more favorable to photochemical O<sub>3</sub> production (see section 5.1). The selection of tropospheric limits 3 km below the tropopause minimized but cannot avoid the influence of transport from stratosphere, the STE process may also contribute to high level of tropospheric O<sub>3</sub> column in spring.

## 4.2 Regional contribution to tropospheric O<sub>3</sub> levels

In order to determine where the air masses came from and thus contributed to the

observed tropospheric O<sub>3</sub> levels, we have used the HYSPLIT (Hybrid Single-Particle Lagrangian Integrated Trajectory) model to calculate the three-dimensional kinematic back trajectories that coincide with the FTS measurements from 2014 - 2017 (Draxler et al., 2009). In the calculation, the GDAS (University of Alaska Fairbanks GDAS Archive) meteorological fields were used with a spatial resolution of 0.25 °× 0.25 °, a time resolution of 6 h and 22 vertical levels from the surface to 250 mbar. All daily back trajectories at 12:00 UTC, with a 24 h pathway arriving at Hefei site at 1500 m a.s.l., have been grouped into clusters, and divided into MAM/JJA and SON/DJF seasons (Stunder, 1996). The results showed that air masses in Jiangsu and Anhui Province in eastern China, Hebei and Shandong Province in northern China, Shaanxi, Henan and Shanxi Province in northwestern China, Hunan and Hubei Province in central China contributed to the observed tropospheric O<sub>3</sub> levels.

In MAM/JJA season (Figure 2(a)), 28.8% of air masses are east origin and arrived at Hefei through the southeast of Jiangsu Province and east of Anhui Province; 41.0% are southwest origin and arrived at Hefei through the northeast of Hunan and Hubei Province, and southwest of Anhui Province; 10.1% are northwest origin and arrived at Hefei through the southeast of Shanxi and Henan Province, and northwest of Anhui Province; 10.1% are north origin and arrived at Hefei through the south of Shandong Province and north of Anhui Province; 10.1% are local origin generated in south of Anhui Province. As a result, air pollution from megacities such as Shanghai, Nanjing, Hangzhou and Hefei in eastern China, Changsha and Wuhan in central-southern China, Zhenzhou and Taiyuan in northwest China, and Jinan in north China could contribute to the observed tropospheric O<sub>3</sub> levels.

In SON/DJF season, trajectories are generally longer and originated in the northwest of the MAM/JJA ones (Figure 2(b)). The direction of air masses originating in the eastern sector shifts from the southeast to northeast of Jiangsu Province, and that of local air masses shifts from the south to the northwest of Anhui province. Trajectories of east origin, west origin, and north origin air masses in SON/DJF are 6.5%, 13.1%, and 0.7% less frequent than the MAM/JJA ones, respectively. As a result, the air masses outside Anhui province have 20.2% smaller contribution to the

observed tropospheric O<sub>3</sub> levels in SON/DJF than in MAM/JJA. In contrast, trajectories of local origin air masses in SON/DJF are 20.2% [more frequent](#) than the MAM/JJA ones, indicating a more significant contribution of air masses inside Anhui province in SON/DJF.

The majority of the Chinese population lives in the eastern part of China, especially in the three most developed regions, the Jing-Jin-Ji (Beijing-Tianjin-Hebei), the Yangtze River Delta (YRD; including Shanghai-Jiangsu-Zhejiang-Anhui), and the Pearl River Delta (PRD; including Guangzhou, Shenzhen, and Hong Kong). These regions consistently have the highest emissions of anthropogenic precursors (Figure S6), which have led to severe region-wide air pollution. Particularly, the Hefei site located in the central-western corner of the YRD, where the population in the southeastern area is typically denser than the northwestern area. Specifically, the southeast of Jiangsu province and the south of Anhui province are two of the most developed areas in YRD, and human activities therein are very intense. Therefore, when the air masses originated from these two areas, O<sub>3</sub> level is usually very high. Overall, compared with SON/DJF season, the more southeastern air masses transportation in MAM/JJA indicated that the observed tropospheric O<sub>3</sub> levels could be more influenced by the densely populated and industrialized areas, [broadly](#) accounting for higher O<sub>3</sub> level and variability in MAM/JJA.

## **5 Tropospheric O<sub>3</sub> production regime**

### **5.1 Meteorological dependency**

Photochemistry in polluted atmospheres, particularly the formation of O<sub>3</sub>, depends not only on pollutant emissions, but also on meteorological conditions (Lei et al., 2008; Wang et al., 2016; Coates et al., 2016). In order to investigate meteorological dependency of O<sub>3</sub> production regime in the observed area, we analyzed the correlation of the tropospheric O<sub>3</sub> with the coincident surface meteorological data. Figure 3 shows time series of temperature, pressure, humidity, and solar radiation recorded by the surface weather station. The seasonal dependencies of all these coincident meteorological elements show no clear



dependencies except for the temperature and pressure which show clear reverse seasonal cycles. Generally, the temperatures are higher and the pressures are lower in MAM/JJA than those in SON/DJF. The correlation plots between FTS tropospheric O<sub>3</sub> column and each meteorological element are shown in Figure 4. The tropospheric O<sub>3</sub> column shows positive correlations with solar radiation, temperature, and humidity, and negative correlations with pressure.

High temperature and strong sunlight primarily affects O<sub>3</sub> production in Hefei in two ways: speeding up the rates of many chemical reactions and increasing emissions of VOCs from biogenic sources (BVOCs) (Sillman and Samson, 1995b). While emissions of anthropogenic VOCs (AVOCs) are generally not dependent on temperature, evaporative emissions of some AVOCs do increase with temperature (Rubin et al., 2006; Coates et al., 2016). Elevated O<sub>3</sub> concentration generally occurs on days with wet condition and low pressure in Hefei probably because these conditions favor the accumulation of O<sub>3</sub> and its precursors. Overall, MAM/JJA meteorological conditions are more favorable to O<sub>3</sub> production (higher sun intensity, higher temperature, wetter condition, and lower pressure) than SON/DJF, which consolidates the fact that tropospheric O<sub>3</sub> in MAM/JJA are larger than those in SON/DJF.

## **5.2 PO<sub>3</sub> relative to CO, HCHO, and NO<sub>2</sub> changes**

In order to determine the relationship between tropospheric O<sub>3</sub> production and its precursors, the chemical sensitivity of PO<sub>3</sub> relative to tropospheric CO, HCHO, and NO<sub>2</sub> changes was investigated. Figure 5 shows time series of tropospheric CO, HCHO, and NO<sub>2</sub> columns that are coincident with O<sub>3</sub> counterparts. The tropospheric NO<sub>2</sub> was deduced from OMI product selected within the  $\pm 0.7^\circ$  latitude/longitude rectangular area around Hefei site. The retrieval uncertainty for tropospheric column of is less than 30% ([https://disc.gsfc.nasa.gov/datasets/OMNO2\\_V003/](https://disc.gsfc.nasa.gov/datasets/OMNO2_V003/)). Tropospheric HCHO and NO<sub>2</sub> show clear reverse seasonal cycles. Generally, tropospheric HCHO are higher and tropospheric NO<sub>2</sub> are lower in MAM/JJA than those in SON/DJF. Pronounced tropospheric CO was observed but the seasonal cycle is not evident probably because

### CO emission is not constant over season or season dependent.

Figure 6 shows the correlation plot between the FTS tropospheric O<sub>3</sub> column and the coincident tropospheric CO, HCHO, and NO<sub>2</sub> columns. The tropospheric O<sub>3</sub> column shows positive correlations with tropospheric CO, HCHO, and NO<sub>2</sub> columns. Generally, the higher the tropospheric CO concentration, the higher the tropospheric O<sub>3</sub>, and both VOCs and NO<sub>x</sub> reductions decrease O<sub>3</sub> production. As an indicator of regional air pollution, the good correlation between O<sub>3</sub> and CO (Figure 6(a)) indicates that the enhancement of tropospheric O<sub>3</sub> is highly associated with the photochemical reactions which occurred in polluted conditions rather than due to the STE process. The relative weaker overall correlations of O<sub>3</sub> with HCHO (Figure 6 (b)) and NO<sub>2</sub> (Figure 6 (c)) are partly explained by different lifetimes of these gases, i.e., several hours to 1 day in summer for NO<sub>2</sub> and HCHO, several days to weeks for O<sub>3</sub>. So older O<sub>3</sub> enhanced air masses easily loose trace of NO<sub>2</sub> or HCHO. Since the sensitivity of PO<sub>3</sub> to VOCs and NO<sub>x</sub> is different under different limitation regimes, the relative flat overall slopes indicates that the O<sub>3</sub> pollution in Hefei can neither be fully attributed to NO<sub>x</sub> pollution nor VOCs pollution.

## **5.3 O<sub>3</sub>-NO<sub>x</sub>-VOCs sensitivities**

### **5.3.1 Transition/ambiguous range estimation**

Referring to previous studies, the chemical sensitivity of PO<sub>3</sub> in Hefei was investigated using the column HCHO/NO<sub>2</sub> ratio (Martin et al., 2004; Duncan et al., 2010; Witte et al., 2011; Choi et al., 2012; Jin and Holloway, 2015; Mahajan et al., 2015; Schroeder et al., 2017; Jin et al., 2017). The methods have been adapted to the particular conditions in Hefei. In particular the findings of Schroeder et.al (2017) have been taken into account.

Since the measurement tools for O<sub>3</sub> and HCHO, the pollution characteristic and the meteorological condition in this study were not the same as those of previous studies, the transition thresholds estimated in either previous studies were not straightly applied here (Martin et al., 2004a; Duncan et al., 2010; Witte et al., 2011; Choi et al., 2012; Jin and Holloway, 2015; Mahajan et al., 2015; Schroeder et al.,

2017; Jin et al., 2017). In order to determine transition thresholds applicable in Hefei, China, we iteratively altered the column HCHO/NO<sub>2</sub> ratio threshold and judged whether the sensitivities of tropospheric O<sub>3</sub> to HCHO or NO<sub>2</sub> changed abruptly. For example, in order to estimate the VOC-limited threshold, we first fitted tropospheric O<sub>3</sub> to HCHO that lies within column HCHO/NO<sub>2</sub> ratios < 2 (an empirical start point) to obtain the corresponding slope, and then we decreased the threshold by 0.1 (an empirical step size) and repeated the fit, i.e., only fitted the data pairs with column HCHO/NO<sub>2</sub> ratios < 1.9. This has been done iteratively. Finally, we sorted out the transition ratio which shows an abrupt change in slope, and regarded this as the VOC-limited threshold. Similarly, the NO<sub>x</sub>-limited threshold was determined by iteratively increasing the column HCHO/NO<sub>2</sub> ratio threshold till the sensitivity of tropospheric O<sub>3</sub> to NO<sub>2</sub> changed abruptly.

The transition threshold estimation with this scheme exploits the fact that O<sub>3</sub> production is more sensitive to VOCs if it is VOCs-limited and is more sensitive to NO<sub>x</sub> if it is NO<sub>x</sub> limited, and it exists a transition point near the threshold (Martin et al., 2004). Su et al. (2017) used this scheme to investigate the O<sub>3</sub>-NO<sub>x</sub>-VOCs sensitivities during the 2016 G20 conference in Hangzhou, China, and argued that this diagnosis of PO<sub>3</sub> could reflect the overall O<sub>3</sub> production conditions.

### **5.3.2 PO<sub>3</sub> limitations in Hefei**

Through the above empirical iterative calculation, we observed a VOC-limited regime with column HCHO/NO<sub>2</sub> ratios < 1.3, a NO<sub>x</sub>-limited regime with column HCHO/NO<sub>2</sub> ratios > 2.8, and a mix VOC-NO<sub>x</sub>-limited regime with column HCHO/NO<sub>2</sub> ratios between 1.3 and 2.8. Column measurements sample a larger portion of the atmosphere, and thus their spatial coverage are larger than in situ measurements. So the photochemical scene disclosed by column measurement is larger than the in-situ measurement. Specifically, this study reflects the mean photochemical condition of the troposphere.

Schroeder et. al. (2017) argued, the column measurements from space have to be used with care because of the high uncertainty and the inhomogeneity of the satellite

measurements. This has been mitigated in this study by the following:

The FTIR measurements have a much smaller footprint than the satellite measurements. Also we concentrate on measurements recorded during midday, when the mixing layer has largely been dissolved.

The measurements are more sensitive to the lower parts of the troposphere, which can be inferred from the normalized AVK's. This reason is simply, that the AVK's show the sensitivity to the column, but the column per altitude decreases with altitude.

Figure 7 shows time series of column HCHO/NO<sub>2</sub> ratios which varied over a wide range from 1.0 to 9.0. The column HCHO/NO<sub>2</sub> ratios in summer are typically larger than those in winter, indicating that the PO<sub>3</sub> is mainly NO<sub>x</sub> limited in summer and mainly VOC limited or mix VOC-NO<sub>x</sub> limited in winter. Based on the calculated transition criteria, 106 days of observations that have coincident O<sub>3</sub>, HCHO, and NO<sub>2</sub> counterparts in the reported period are classified, where 57 days (53.8%) are in MAM/JJA season and 49 days (46.2%) are in SON/DJF season. Table 4 listed the statistics for the 106 days of observations, which shows that NO<sub>x</sub> limited, mix VOC-NO<sub>x</sub> limited, and VOC limited PO<sub>3</sub> accounts for 60.3% (64 days), 28.3% (30 days), and 11.4% (12 days), respectively. The majority of NO<sub>x</sub> limited (70.3%) PO<sub>3</sub> lies in MAM/JJA season, while the majorities of mix VOC-NO<sub>x</sub> limited (70%) and VOC limited (75%) PO<sub>3</sub> lie in SON/DJF season. As a result, reductions in NO<sub>x</sub> and VOC could be more effective to mitigate O<sub>3</sub> pollution in MAM/JJA and SON/DJF season, respectively. Furthermore, considering most of PO<sub>3</sub> are NO<sub>x</sub> limited or mix VOC-NO<sub>x</sub> limited, reductions in NO<sub>x</sub> would reduce O<sub>3</sub> pollution in eastern China.

## 6 Conclusion

We investigated the seasonal evolution and photochemical production regime of tropospheric O<sub>3</sub> in eastern China from 2014 – 2017 by using tropospheric O<sub>3</sub>, CO and HCHO columns derived from Fourier transform infrared spectrometry (FTS), tropospheric NO<sub>2</sub> column deduced from Ozone Monitoring Instrument (OMI), the surface meteorological data, and a back trajectory cluster analysis technique. A pronounced seasonal cycle for tropospheric O<sub>3</sub> is captured by the FTS, which roughly

increases over time at the first half year and reaches the maximum in June, and then it decreases over time at the second half year. Tropospheric O<sub>3</sub> columns in June are  $1.55 \times 10^{18}$  molecules\*cm<sup>-2</sup> (56 DU (Dobson Units)) and in December are  $1.05 \times 10^{18}$  molecules\*cm<sup>-2</sup> (39 DU). Tropospheric O<sub>3</sub> columns in June were ~ 50% higher than those in December. A broad maximum within both spring and summer (MAM/JJA) is observed and the day-to-day variations in MAM/JJA are generally larger than those in autumn and winter (SON/DJF). This differs from tropospheric O<sub>3</sub> measurements in Vigouroux et al. (2015). However, Vigouroux et al. (2015) used measurements at relatively clean sites.

Back trajectories analysis showed that air pollution in Jiangsu and Anhui Province in eastern China, Hebei and Shandong Province in northern China, Shaanxi, Henan and Shanxi Province in northwest China, Hunan and Hubei Province in central China contributed to the observed tropospheric O<sub>3</sub> levels. Compared with SON/DJF season, the observed tropospheric O<sub>3</sub> levels in MAM/JJA are more influenced by transport of air masses from densely populated and industrialized areas, and the high O<sub>3</sub> level and variability in MAM/JJA is determined by the photochemical O<sub>3</sub> production. The tropospheric column HCHO/NO<sub>2</sub> ratio is used as a proxy to investigate the chemical sensitivity of O<sub>3</sub> production rate (PO<sub>3</sub>). The results show that the PO<sub>3</sub> is mainly nitrogen oxide (NO<sub>x</sub>) limited in MAM/JJA, while it is mainly VOC or mix VOC-NO<sub>x</sub> limited in SON/DJF. Reductions in NO<sub>x</sub> and VOC could be more effective to mitigate O<sub>3</sub> pollution in MAM/JJA and SON/DJF season, respectively. Considering most of PO<sub>3</sub> are NO<sub>x</sub> limited or mix VOC-NO<sub>x</sub> limited, reductions in NO<sub>x</sub> would reduce O<sub>3</sub> pollution in eastern China.

## **Acknowledgements**

This work is jointly supported by the National High Technology Research and Development Program of China (No. 2016YFC0200800, No. 2017YFC0210002, No. 2016YFC0203302), the National Science Foundation of China (No. 41605018, No.41877309, No. 41405134, No.41775025, No. 41575021, No. 51778596, No. 91544212, No. 41722501, No. 51778596), Anhui Province Natural Science

Foundation of China (No. 1608085MD79), Outstanding Youth Science Foundation (No. 41722501) and the German Federal Ministry of Education and Research (BMBF) (Grant No. 01LG1214A). The processing and post processing environment for SFIT4 are provided by National Center for Atmospheric Research (NCAR), Boulder, Colorado, USA. The NDACC networks are acknowledged for supplying the SFIT software and advice. The HCHO micro-windows were obtained at BIRA-IASB during the ESA PRODEX project TROVA (2016-2018) funded by the Belgian Science Policy Office. The LINEFIT code is provided by Frank Hase, Karlsruhe Institute of Technology (KIT), Institute for Meteorology and Climate Research (IMK-ASF), Germany. The authors acknowledge the NOAA Air Resources Laboratory (ARL) for making the HYSPLIT transport and dispersion model available on the Internet. The authors would also like to thank Dr. Jason R. Schroeder and three anonymous referees for useful comments that improved the quality of this paper.

## References

- Albrecht T., Notholt J., Wolke R., Solberg S., Dye C., Malberg H., Variations of  $\text{CH}_2\text{O}$  and  $\text{C}_2\text{H}_2$  determined from ground based FTIR measurements and comparison with model results, *Adv. Space Res.*, 29, p. 1713-1718, 2002.
- Boersma, K. F., D. J. Jacob, M. Trainic, Y. Rudich, I. DeSmedt, R. Dirksen, and H. J. Eskes (2009), Validation of urban  $\text{NO}_2$  concentrations and their diurnal and seasonal variations observed from the SCIAMACHY and OMI sensors using in situ surface measurements in Israeli cities, *Atmos. Chem. Phys.*, 9(12), 3867–3879, doi:10.5194/acp-9-3867-2009.
- Choi, Y., H. Kim, D. Tong, and P. Lee (2012), Summertime weekly cycles of observed and modeled  $\text{NO}_x$  and  $\text{O}_3$  concentrations as a function of satellite-derived ozone production sensitivity and land use types over the continental United States, *Atmos. Chem. Phys.*, 12(14), 6291–6307, doi:10.5194/acp-12-6291-2012.
- Coates J., Mar K. A., Ojha N., Butler T. M.. The influence of temperature on ozone production under varying  $\text{NO}_x$  conditions - a modelling study. *Atmospheric Chemistry and Physics*. 2016,16(18):11601-15.

- Duncan, B.N., et al., 2010. Application of OMI observations to a space-based indicator of NO<sub>x</sub> and VOC controls on surface ozone formation. *Atmos. Environ.* 44, 2213-2223.
- Draxler, R. R., Stunder, B., Rolph, G., and Taylor, A.: HYSPLIT\_4 User's Guide, via NOAA ARL website. NOAA Air Resources Laboratory, Silver Spring, MD, December 1997, revised January 2009, [http://www.arl.noaa.gov/documents/reports/hysplit\\_user\\_guide.pdf](http://www.arl.noaa.gov/documents/reports/hysplit_user_guide.pdf) (last access: 19 May 2017), 2009.
- Edwards, P. M., Young, C. J., Aikin, K., & Degouw, J. A. (2013). Ozone photochemistry in an oil and natural gas extraction region during winter: simulations of a snow-free season in the Uintah basin, Utah. *Atmospheric Chemistry & Physics*, 13(17), 8955-8971.
- Franco B., Hendrick F., Van Roozendaal M., Muller J. F., Stavrou T., Marais E. A., Retrievals of formaldehyde from ground-based FTIR and MAX-DOAS observations at the Jungfraujoch station and comparisons with GEOS-Chem and IMAGES model simulations. *Atmospheric Measurement Techniques*. 2015, 8(4):1733-56.
- Gardiner, T., Forbes, A., de Mazière, M., Vigouroux, C., Mahieu, E., Demoulin, P., Velasco, V., Notholt, J., Blumenstock, T., Hase, F., Kramer, I., Sussmann, R., Stremme, W., Mellqvist, J., Strandberg, A., Ellingsen, K., and Gauss, M.: Trend analysis of greenhouse gases over Europe measured by a network of ground-based remote FTIR instruments, *Atmos. Chem. Phys.*, 8, 6719–6727, doi:10.5194/acp-8-6719-2008, 2008.
- Hase, F.: Improved instrumental line shape monitoring for the ground-based, high-resolution FTIR spectrometers of the Network for the Detection of Atmospheric Composition Change, *Atmos. Meas. Tech.*, 5, 603–610, doi:10.5194/amt-5-603-2012, 2012.
- Jin, X., and T. Holloway (2015), Spatial and temporal variability of ozone sensitivity over China observed from the Ozone Monitoring Instrument, *J. Geophys. Res. Atmos.*, 120, 7229–7246, doi:10.1002/2015JD023250.
- Jin X. M., Fiore A.M., Murray L.T., Valin L.C., Lamsal L.N., Duncan B. Evaluating a

- Space-Based Indicator of Surface Ozone-NO<sub>x</sub>-VOC Sensitivity Over Midlatitude Source Regions and Application to Decadal Trends. *J Geophys Res-Atmos.* 2017,122(19):10231-53.
- Jones N.B., Riedel K., Allan W., Wood S., Palmer P.I., Chance K., et al. Long-term tropospheric formaldehyde concentrations deduced from ground-based fourier transform solar infrared measurements. *Atmos Chem Phys.* 2009,9(18):7131-42.
- Kleinman, L., Daum, P., Lee, Y.-N., Nunnermacker, L., Springston, S., Weinstein-Lloyd, J., Rudolph, J., 2005. A comparative study of ozone production in five U.S. metropolitan areas. *Journal of Geophysical Research* 110, D02301. doi:10.1029/2004JD005096.
- Kalnay E., Kanamitsu M., Kistler R., et al. (1996) The NCEP/NCAR 40-year reanalysis project. *Bulletin of the American Meteorological Society*, 77, 437-472.
- Lei W., Zavala M., de Foy B., Volkamer R., Molina L. T.. Characterizing ozone production and response under different meteorological conditions in Mexico City. *Atmospheric Chemistry and Physics.* 2008, 8(24):7571-81.
- Martin, R., Fiore, A., Van Donkelaar, A., 2004a. Space-based diagnosis of surface ozone sensitivity to anthropogenic emissions. *Geophysical Research Letters* 31, L06120. doi:10.1029/2004GL019416.
- Martin, R., Parrish, D., Ryerson, T., Nicks, D., Chance, K., Kurosu, T., Jacob, D., Sturges, E., Fried, A., Wert, B., 2004b. Evaluation of GOME satellite measurements of tropospheric NO<sub>2</sub> and HCHO using regional data from aircraft campaigns in the southeastern United States. *Journal of Geophysical Research* 109, D24307. doi:10.1029/2004JD004869.
- Millet, D. B., D. J. Jacob, K. F. Boersma, T.-M. Fu, T. P. Kurosu, K. Chance, C. L. Heald, and A. Guenther (2008), Spatial distribution of isoprene emissions from North America derived from formaldehyde column measurements by the OMI satellite sensor, *J. Geophys. Res.*, 113, D02307, doi:10.1029/2007JD008950.
- Mahajan, A. S., I. De Smedt, M. S. Biswas, S. Ghude, S. Fadnavis, C. Roy, and M. van Roozendaal (2015), Inter-annual variations in satellite observations of nitrogen dioxide and formaldehyde over India, *Atmos. Environ.*, 116, 194–201,



doi:10.1016/j.atmosenv.2015.06.004.

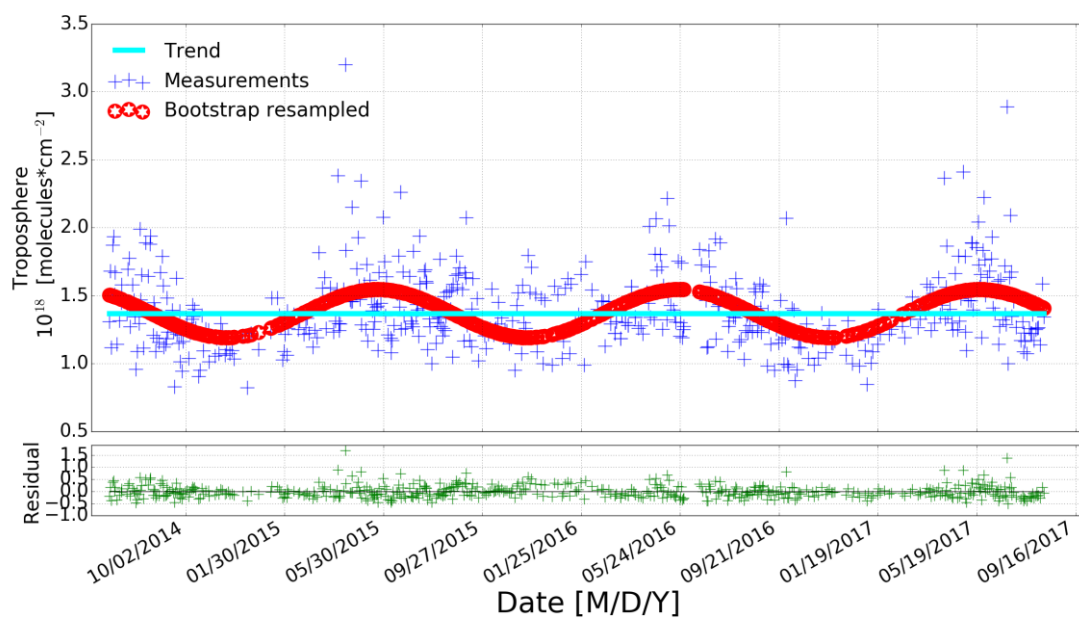
- Oltmans S. J., Lefohn A. S., Harris J. M., et al. Long-term changes in tropospheric ozone. *Atmospheric Environment*, 2006, 40(17):3156-3173.
- Rothman, L. S., Gordon, I. E., Barbe, A., Benner, D. C., Bernath, P. F., Birk, M., Boudon, V., Brown, L. R., Campargue, A., Champion, J.-P., Chance, K., Coudert, L. H., Danaj, V., Devi, V. M., Fally, S., Flaud, J.-M., Gamache, R. R., Goldman, A., Jacquemart, D., Kleiner, I., Lacome, N., Lafferty, W. J., Mandin, J.-Y., Massie, S. T., Mikhailenko, S. N., Miller, C. E., Moazzen-Ahmadi, N., Naumenko, O. V., Nikitin, A. V., Orphal, J., Perevalov, V. I., Perrin, A., Predoi-Cross, A., Rinsland, C. P., Rotger, M., Šime. cková, M., Smith, M. A. H., Sung, K., Tashkun, S. A., Tennyson, J., Toth, R. A., Vandaele, A. C., and Vander Auwera, J.: The Hitran 2008 molecular spectroscopic database, *J. Quant. Spectrosc. Ra.*, 110, 533–572, 2009.
- Rubin, J. I., Kean, A. J., Harley, R. A., Millet, D. B., and Goldstein, A. H.: Temperature dependence of volatile organic compound evaporative emissions from motor vehicles, *J. Geophys. Res.-Atmos.*, 111, d03305, doi:10.1029/2005JD006458, 2006.
- Schroeder, J. R., Crawford, J. H., Fried, A., Walega, J., Weinheimer, A., & Wisthaler, A., et al. (2017). New insights into the column CH<sub>2</sub>O/NO<sub>2</sub> ratio as an indicator of near - surface ozone sensitivity. *Journal of Geophysical Research Atmospheres*, 122(16).
- Sillman, S., 1995a. The use of NO<sub>y</sub>, H<sub>2</sub>O<sub>2</sub>, and HNO<sub>3</sub> as indicators for ozone-NO<sub>x</sub> hydrocarbon sensitivity in urban locations. *J. Geophys. Res.* 100, 14175-14188.
- Sillman, S. and Samson, P. J.: Impact of temperature on oxidant photochemistry in urban, polluted rural and remote environments, *J. Geophys. Res.-Atmos.*, 100, 11497–11508, 1995b.
- Stunder, B.: An assessment of the Quality of Forecast Trajectories, *J. Appl. Meteorol.*, 35, 1319–1331, 1996.
- Streets, D. G., et al. (2013), Emissions estimation from satellite retrievals: A review of current capability, *Atmos. Environ.*, 77, 1011–1042, doi:10.1016/j.atmosenv.

2013.05.051.

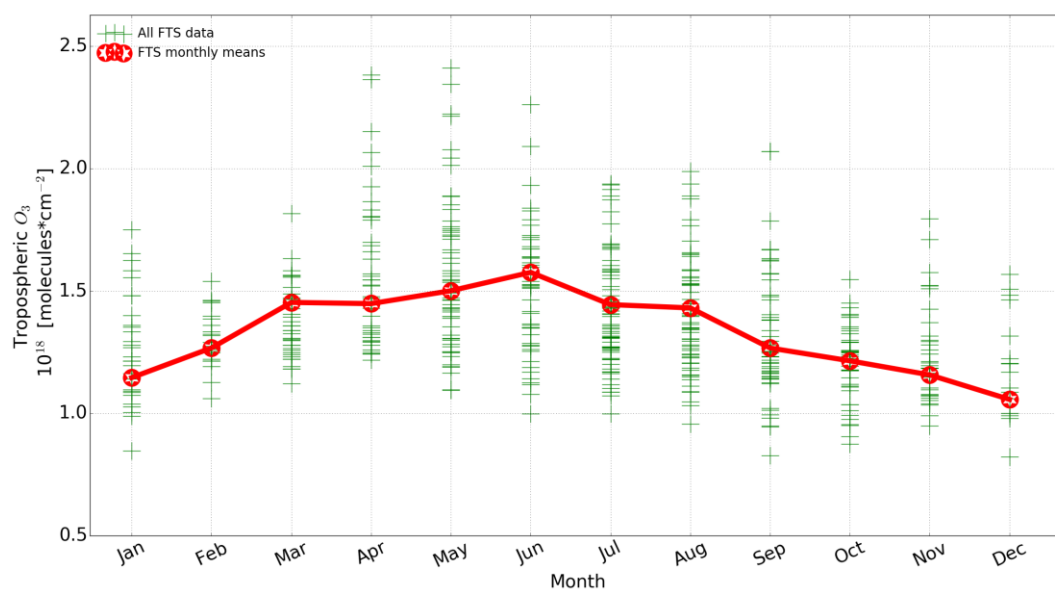
- Su W. J., Liu C., Hu Q.H., Fan G.Q., Xie Z.Q., Huang X., Characterization of ozone in the lower troposphere during the 2016 G20 conference in Hangzhou. *Sci Rep-Uk*. 2017,7.
- Tang, G., Wang, Y., Li, X., Ji, D., & Gao, X. (2011). Spatial-temporal variations of surface ozone and ozone control strategy for northern china. *Atmospheric Chemistry & Physics*, 11(9), 26057-26109.
- Tonnesen, G. S., and R. L. Dennis (2000), Analysis of radical propagation efficiency to assess ozone sensitivity to hydrocarbons and NO<sub>2</sub>. Long-lived species as indicators of ozone concentration sensitivity, *J. Geophys. Res.*, 105(D7), 9227–9241, doi:10.1029/1999JD900372.
- Tian Y., Sun Y.W., Liu C., Wang W., Shan C. G., Xu X.W., Hu Q.H., Characterisation of methane variability and trends from near-infrared solar spectra over Hefei, China, *Atmospheric Environment*, Volume 173, 2018, Pages 198-209, ISSN 1352-2310, <https://doi.org/10.1016/j.atmosenv.2017.11.001>.
- Vigouroux, C., Blumenstock, T., Coffey, M., Errera, Q., Garc á, O., Jones, N. B., Hannigan, J. W., Hase, F., Liley, B., Mahieu, E., Mellqvist, J., Notholt, J., Palm, M., Persson, G., Schneider, M., Servais, C., Smale, D., Thölix, L., and De Mazi ère, M.: Trends of ozone total columns and vertical distribution from FTIR observations at eight NDACC stations around the globe, *Atmos. Chem. Phys.*, 15, 2915-2933, doi:10.5194/acp-15-2915-2015, 2015.
- Vigouroux C., Hendrick F, Stavrakou T, et al. Ground-based FTIR and MAX-DOAS observations of formaldehyde at Réunion Island and comparisons with satellite and model data[J]. *Atmospheric Chemistry & Physics*, 2009, 9(4):9523-9544.
- Vigouroux, C., Bauer Aquino, C. A., Bauwens, M., Becker, C., Blumenstock, T., De Mazi ère, M., Garc á, O., Grutter, M., Guarin, C., Hannigan, J., Hase, F., Jones, N., Kivi, R., Koshelev, D., Langerock, B., Lutsch, E., Makarova, M., Metzger, J.-M., Müller, J.-F., Notholt, J., Ortega, I., Palm, M., Paton-Walsh, C., Poberovskii, A., Rettinger, M., Robinson, J., Smale, D., Stavrakou, T., Stremme, W., Strong, K., Sussmann, R., T é Y., and Toon, G.: NDACC harmonized

- formaldehyde time series from 21 FTIR stations covering a wide range of column abundances, *Atmos. Meas. Tech.*, 11, 5049-5073, <https://doi.org/10.5194/amt-11-5049-2018>, 2018.
- Witte, J.C., Duncan, B.N, Douglass, A.R, Kurosu, T.P, Chance, K et al. "The unique OMI HCHO/NO<sub>2</sub> feature during the 2008 Beijing Olympics: Implications for ozone production sensitivity". *Atmospheric Environment*. 45.18 2011-06-01. 3103(9).
- Viatte C., Strong K., Walker K.A., Drummond J.R. Five years of CO, HCN, C<sub>2</sub>H<sub>6</sub>, C<sub>2</sub>H<sub>2</sub>, CH<sub>3</sub>OH, HCOOH and H<sub>2</sub>CO total columns measured in the Canadian high Arctic. *Atmospheric Measurement Techniques*. 2014;7(6):1547-70.
- Wennberg, P. O., and Dabdub D. Atmospheric chemistry. Rethinking ozone production. *Science* 319.5870(2008):1624.
- Wang T., Xue L. K., Brimblecombe P., Lam Y. F., Li. L., Zhang L. Ozone pollution in China: A review of concentrations, meteorological influences, chemical precursors, and effects. *Sci Total Environ*. 2017, 575:1582-96.
- Wang W., Tian Y., Liu C., Sun Y., Liu W., Xie P., et al. Investigating the performance of a greenhouse gas observatory in Hefei, China. *Atmos Meas Tech*. 2017,10(7):2627-43.
- Xing, C., Liu, C., Wang, S., Chan, K. L., Gao, Y., & Huang, X., et al. (2017). Observations of the vertical distributions of summertime atmospheric pollutants and the corresponding ozone production in shanghai, china. *Atmospheric Chemistry & Physics*, 17(23), 1-31.

## Figs

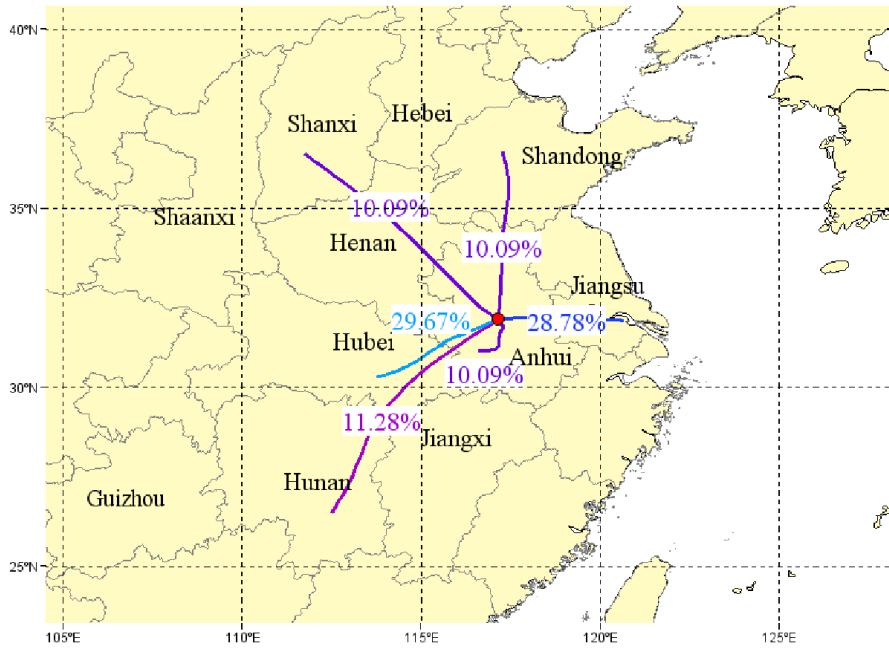


(a)

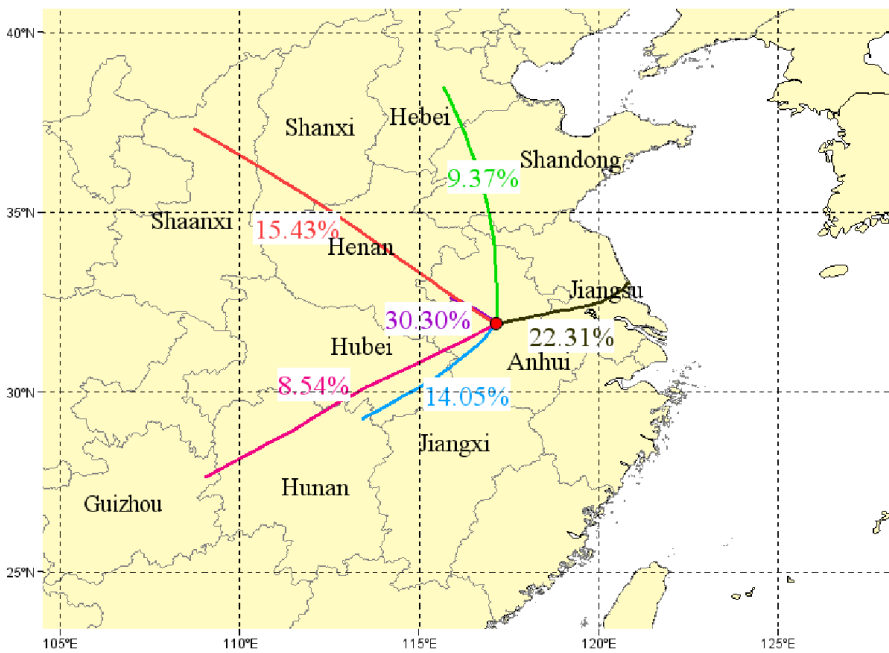


(b)

Figure 1. (a): FTS measured and bootstrap resampled tropospheric  $O_3$  columns at Hefei site. The linear trend and the residual are also shown. [Detailed description of the bootstrap method can be found in Gardiner et al., 2008.](#) (b): Tropospheric  $O_3$  column monthly means derived from (a).



(a)



(b)

Figure 2. One-day HYSPLIT back trajectory clusters arriving at Hefei at 1500 m a.s.l that are coincident with the FTS measurements from 2014 - 2017. (a) Spring and summer (MAM/JJA), and (b) Autumn and winter (SON/DJF) season. The base map was generated using the TrajStat 1.2.2 software (<http://www.meteothinker.com>).

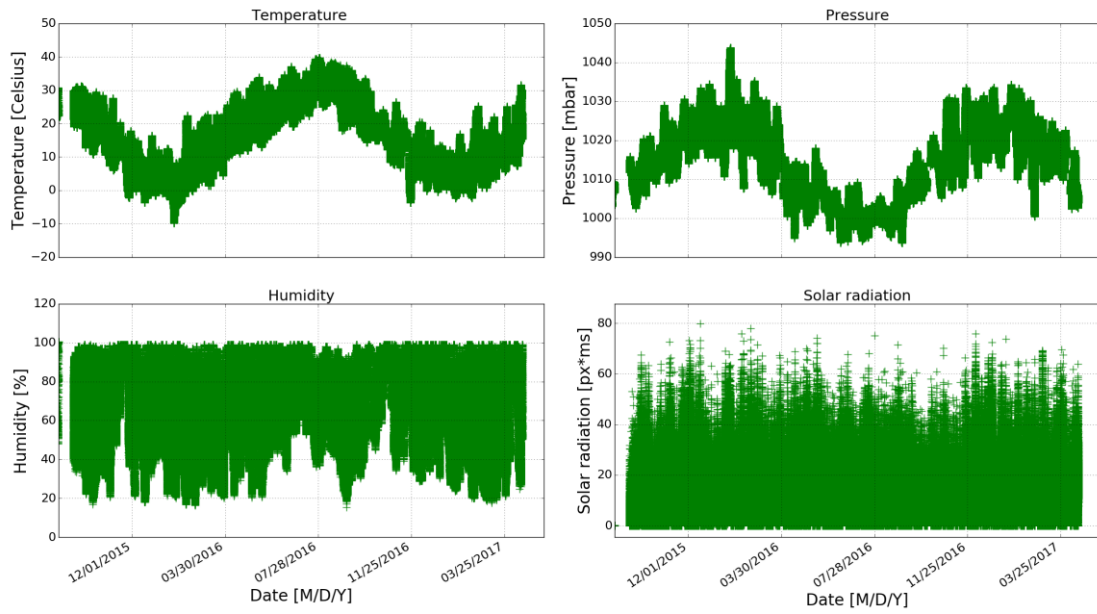


Figure 3. Minutely averaged time series of temperature, pressure, humidity, and solar radiation recorded by the surface weather station.

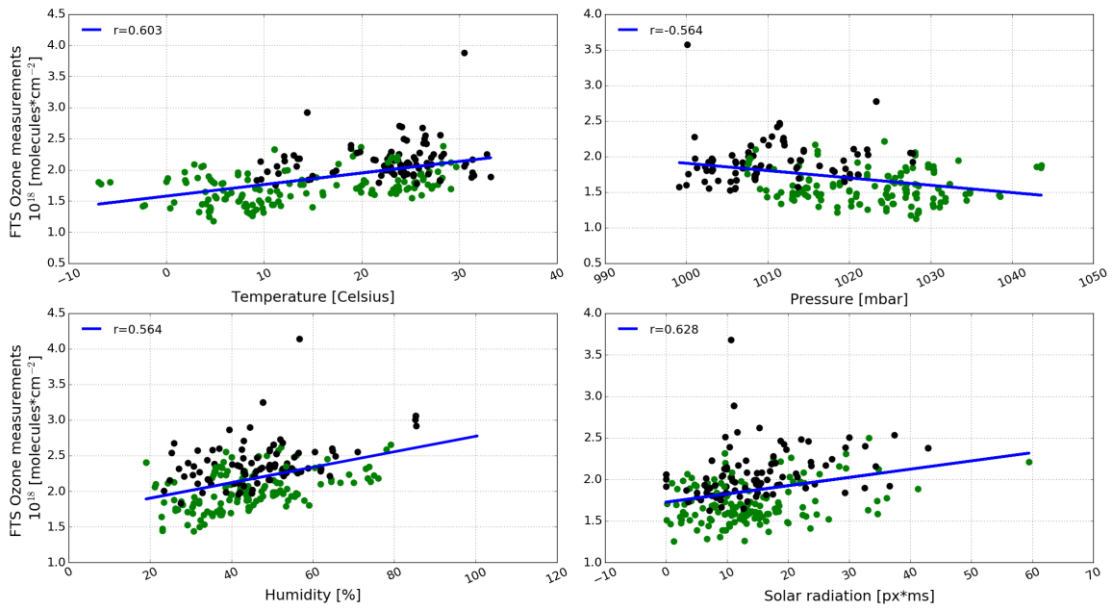


Figure 4. Correlation plot between the FTS tropospheric O<sub>3</sub> column and the coincident surface meteorological data. Black dots are data pairs within MAM/JJA season and green dots are data pairs within SON/DJF season.

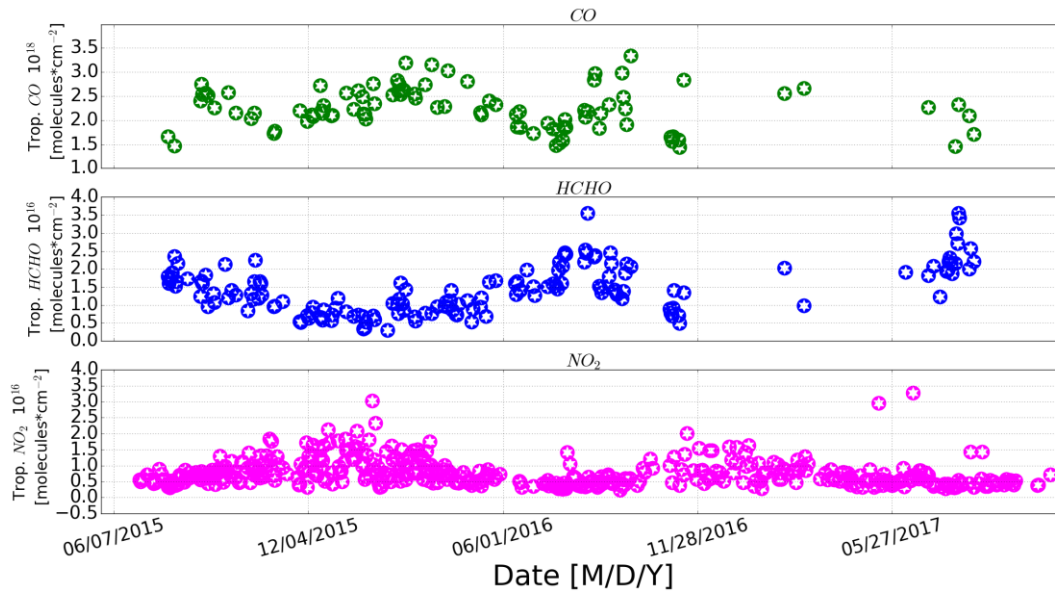


Figure 5. Time series of tropospheric CO, HCHO, and NO<sub>2</sub>. Tropospheric CO and HCHO were derived from FTS observations which is the same as tropospheric O<sub>3</sub> and tropospheric NO<sub>2</sub> is derived from OMI data.

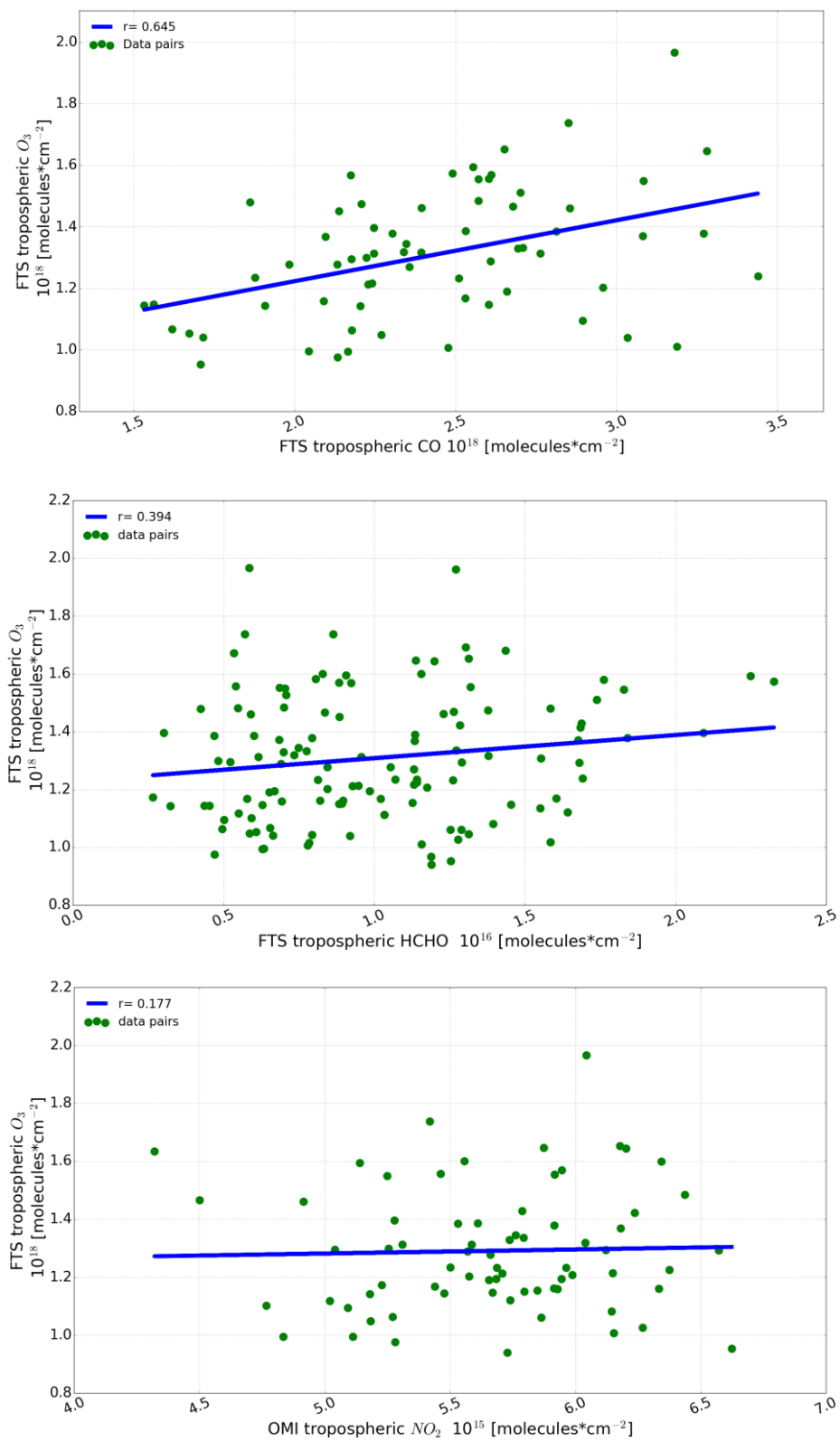


Figure 6. Correlation plot between the FTS tropospheric  $O_3$  column and coincident tropospheric CO (upper), HCHO (middle), and  $NO_2$  (bottom) columns. The CO and HCHO data are retrieved from FTS observations and the  $NO_2$  data were deduced from OMI product.



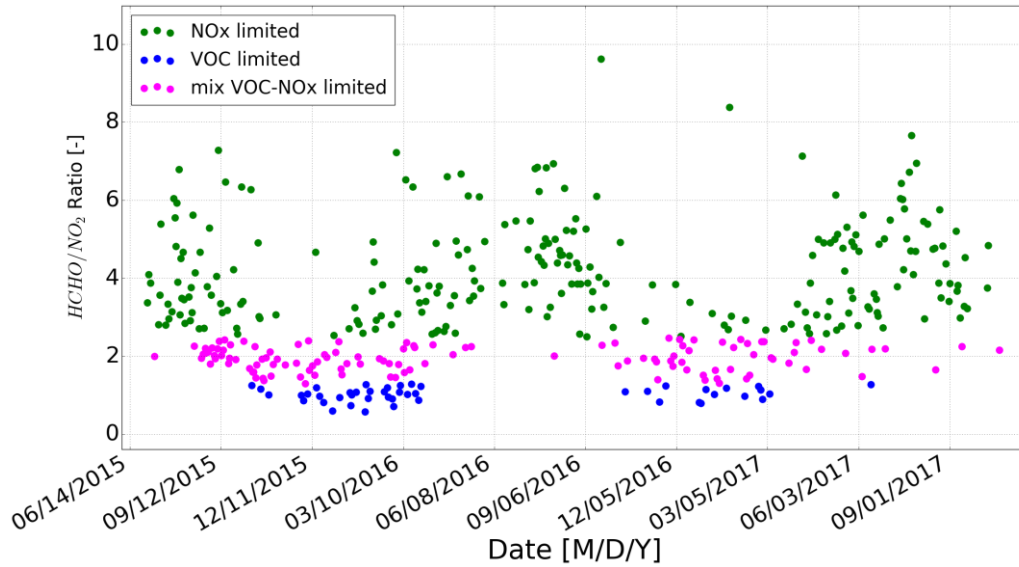


Figure 7. Time series of column HCHO/NO<sub>2</sub> ratios.

## Tables

Table 1. Summary of the retrieval parameters used for O<sub>3</sub>, CO, and HCHO. All micro windows (MW) are given in cm<sup>-1</sup>.

Gases		O <sub>3</sub>	CO	HCHO
Retrieval code		SFIT4 v 0.9.4.4	SFIT4 v 0.9.4.4	SFIT4 v 0.9.4.4
Spectroscopy		HITRAN2008	HITRAN2008	HITRAN2008
P, T, H <sub>2</sub> O profiles		NCEP	NCEP	NCEP
A priori profiles for target/interfering gases except H <sub>2</sub> O		WACCM	WACCM	WACCM
MW for profile retrievals		1000-1004.5	2057.7-2058 2069.56-2069.76 2157.5-2159.15	2763.42-2764.17 2765.65-2766.01 2778.15-2779.1 2780.65-2782.0
Retrieved interfering gases		H <sub>2</sub> O, CO <sub>2</sub> , C <sub>2</sub> H <sub>4</sub> , <sup>668</sup> O <sub>3</sub> , <sup>686</sup> O <sub>3</sub>	O <sub>3</sub> , N <sub>2</sub> O, CO <sub>2</sub> , OCS, H <sub>2</sub> O	CH <sub>4</sub> , O <sub>3</sub> , N <sub>2</sub> O, HDO
SNR for de-weighting		None	500	600
Regularization	S <sub>a</sub>	Diagonal: 20% No correlation	Diagonal: 11% ~ 27% No correlation	Diagonal: 10% No correlation
	S <sub>e</sub>	Real SNR	Real SNR	Real SNR
ILS		LINEFIT145	LINEFIT145	LINEFIT145
Error analysis		Systematic error: -Smoothing error (smoothing) -Errors from other parameters: Background curvature (curvature), Optical path difference (max_opd), Field of view (omega), Solar line strength (solstrnth), Background slope (slope), Solar line shift (solshft), Phase (phase), Solar zenith angle(sza), Line temperature broadening (linetair_gas), Line pressure broadening (linepair_gas), Line intensity(lineint_gas) Random error: -Interference errors: retrieval parameters (retrieval_parameters), interfering species (interfering_species) -Measurement error (measurement) - Errors from other parameters: Temperature (temperature), Zero level (zshift)		

Table 2. Typical degrees of freedom for signal (DOFs) and sensitive range of the retrieved O<sub>3</sub>, CO, and HCHO profiles at Hefei site.

Gas	Total column DOFs	Sensitive range (km)	Tropospheric partial column (km)	Tropospheric DOFs
O <sub>3</sub>	4.8	Ground - 44	Ground - 12	1.3
CO	3.5	Ground - 27	Ground - 12	2.7
HCHO	1.2	Ground - 18	Ground - 12	1.1

Table 3. Errors in % of the column amount of O<sub>3</sub>, CO, and HCHO for 0–12 km tropospheric partial column and for the total column.

Gas	O <sub>3</sub>		CO		HCHO	
	Altitude (km)	Total column	Altitude (km)	Total column	Altitude (km)	Total column
Total random	0–12	0.59	0–12	0.66	0–12	0.97
Total systematic	8.1	4.86	5.7	3.9	9.6	5.7
Total errors	8.7	5.0	6.8	3.95	10.2	5.8

Table 4. Chemical sensitivities of PO<sub>3</sub> for the selected 106 days of observations that have coincident O<sub>3</sub>, HCHO, and NO<sub>2</sub> counterparts

Items	Proportion		Autumn and winter		Spring and summer	
	days	percentage	days	percentage	days	percentage
NO <sub>x</sub> limited	64	60.3%	19	29.7%	45	70.3%
Mix VOC-NO <sub>x</sub> limited	30	28.3%	21	70%	9	30%
VOC limited	12	11.4%	9	75%	3	25%
Sum	106	100%	49	46.2%	57	53.8%